Check for updates

Original Research Article

Formulation and Evaluation of Polyherbal Silver Nanoparticle-loaded Thermosensitive Poloxamer Gel for Acute Wound Healing

Pharmacognosy Magazine
22(4) 1627–1638, 2026
© The Author(s) 2026
Article reuse guidelines:
in.sagepub.com/journals-permissions-india
DOI: 10.1177/09731296261466063
journals.sagepub.com/home/phm

Predeepkumar Narayanappa Shiroorka[1], Yogesh Kumar S[2], Sowmya[2], Prakash Goudanavar[2], Nimbagal Raghavendra Naveen [2], Vedamurthy Joshi[2], Girish Meravanige[1], Krishna Swaroop[1] and Nagaraja Sreeharsha[3]

Abstract

Background: Wound healing is a dynamic, multistage biological process involving hemostasis, inflammation, proliferation, and remodeling. Despite advances in wound care, effective management of acute wounds remains a challenge. Medicinal plants such as *Curcuma longa, Morinda citrifolia, Tridax procumbens*, and *Lantana camara* possess antioxidant and anti-inflammatory properties that support tissue repair.

Objectives: This study aimed to enhance wound healing efficacy by synthesizing polyherbal silver nanoparticles (AgNPs) and incorporating them into a thermosensitive gel system.

Materials and Methods: Polyherbal extracts were prepared using steam distillation followed by maceration and evaluated for phytochemical composition and antioxidant activity. AgNPs were synthesized using the herbal extracts and silver nitrate. The AgNPs were characterized by UV–visible spectrophotometry, Fourier transform infrared (FTIR) spectroscopy, particle size analysis, and zeta potential measurement. A thermosensitive gel was formulated using Poloxamer 407 and loaded with varying concentrations of polyherbal AgNPs. Physicochemical properties were evaluated. *In vitro* wound healing activity was assessed using C2C12 murine myoblast cell lines, while *in vivo* efficacy was evaluated using an excision wound model in male Wistar albino rats.

Results: The optimized AgNP formulation exhibited a mean particle size of 111.27 ± 3.36 nm and a zeta potential of −11.13 ± 0.8 mV, indicating moderate stability. The AgNP-loaded gels showed acceptable physicochemical properties. *In vitro* studies demonstrated concentration-dependent enhancement of cell migration, with the 10% AgNP-loaded gel showing the highest wound closure. *In vivo* studies revealed that the 10% polyherbal AgNP-loaded gel achieved 95.18% wound contraction within 15 days, significantly outperforming other formulations.

Conclusion: A polyherbal AgNP-loaded thermosensitive gel significantly enhanced wound healing *in vitro* and *in vivo*, highlighting its potential as a promising therapeutic approach for acute wound management.

Keywords

Antioxidant activity, excision wound model, polyherbal extract, silver nanoparticles, thermosensitive gel, wound healing

Received 24 April 2025; **revised** 03 March 2026; **accepted** 16 March 2026

Introduction

The skin, the first and outermost barrier, is responsible for initiating the synthesis of vitamin D, protecting against harmful UV rays, and promoting thermoregulation (Rodrigues et al., 2019). A wound is defined as the loss of a cell's structural and functional integrity caused by physical, microbial, chemical, thermal, and other factors (Sharma et al., 2021). Wound healing is a multistep process with four stages: hemostasis, inflammation, proliferation, and remodeling. Hemostasis is the initial phase of wound healing. Blood vessel constriction quickly stops bleeding after a wound. The

[1]Department of Biomedical Sciences, College of Medicine, King Faisal University, Al-Ahsa, Saudi Arabia
[2]Department of Pharmaceutics, Sri Adichunchanagiri College of Pharmacy, Adichunchanagiri University, Mandya, Karnataka, India
[3]Department of Pharmaceutical Sciences, College of Clinical Pharmacy, King Faisal University, Al-Ahsa, Saudi Arabia

Corresponding authors:
Vedamurthy Joshi, Department of Pharmaceutics, Sri Adichunchanagiri College of Pharmacy, B G Nagara, Mandya, Karnataka 571418, India.
E-mail: vedamurthyjoshi@gmail.com
Predeepkumar Narayanappa Shiroorka, Department of Biomedical Sciences, College of Medicine, King Faisal University, Al-Ahsa 31982, Saudi Arabia.
E-mail: pshiroorkar@kfu.edu.sa

Creative Commons Non Commercial CC BY-NC: This article is distributed under the terms of the Creative Commons Attribution-NonCommercial 4.0 License (http://www.creativecommons.org/licenses/by-nc/4.0/) which permits non-Commercial use, reproduction and distribution of the work without further permission provided the original work is attributed as specified on the SAGE and Open Access pages (https://us.sagepub.com/en-us/nam/open-access-at-sage).

inflammatory stage follows the hemostasis phase. Fibrin clots will degrade, and capillaries will become permeable, allowing macrophages and neutrophils to enter the injury site and activate the complement system. These neutrophils engage in the wound immediately after injury and reach their maximum within 24–48 h (Wilkinson & Hardman, 2020).

Fibroblasts migrate into the wound space for the synthesis of new collagen fibers (Kordestani, 2019).

The longest period of wound healing, lasting anywhere from 21 days to a year, is called remodeling. This phase is characterized by the wound contracting and the collagen rearranging. The process of wound healing is impacted by several factors, including age, infections, stress, and chronic illnesses such as autoimmune diseases in one or the other way (Kordestani, 2019).

Since the beginning of time, people have utilized herbs and natural remedies to treat wounds. Many plant sources are used for wound healing, including *Curcuma longa, Lantana camara, Azadirachta indica, Tridax procumbens, Morinda citrifolia*, and *Glycyrrhiza glabra* (Kumar et al., 2007). The well-known traditional medicinal plant *C. longa* is well-known for its ability to reduce inflammation, boost antioxidant levels, and heal wounds. It has long been grown in India and may have anti-inflammatory, antioxidant, and wound-healing properties (Jyotirmayee & Mahalik, 2022). *C. longa* silver nanoparticles (AgNPs) have also shown potent wound healing capabilities, and nanoformulations of the extracts of the same have yielded positive results across the research spectrum (Irham & Hardiyanti, 2021; Raghupathy et al., 2017). *M. citrifolia* has been utilized across the globe for its anti-inflammatory properties. *M. citrifolia* shows potential reduction of inflammatory mediators such as TNF-α, IL-1, and NO levels (Coutinho de Sousa et al., 2017). *T. procumbens* is a local weed that has the potential for wound healing and anti-inflammatory activity. It has been formulated into AgNPs, hemostatic films, and even the raw extract of the plant material has also shown potential wound-healing properties (Fatima et al., 2021; Ravindran et al., 2019; Yaduvanshi et al., 2011).

Polyethene oxide and polypropylene oxide groups copolymerize to generate poloxamers, which are hydrophilic non-ionic copolymers. Surface-active characteristics are imparted by these blocks. Poloxamers have been utilized for a variety of drug delivery systems and tissue regeneration scaffolds because of their thermoreversible qualities and capacity for tissue regeneration, mostly because of their wound-healing qualities (Russo & Villa, 2019).

This work uses four distinct plant sources: *C. longa, M. citrifolia, T. procumbens*, and *L. camara*, and investigates their potential for wound healing by combining them into a polyherbal gel that is loaded with AgNPs. The gelling agent used in this study is Poloxamer 407, and the wound healing effect is examined. A limitation of this study is the lack of histological evaluation, which could have provided direct visual confirmation of tissue regeneration. Future studies will incorporate histological analysis to strengthen the mechanistic understanding of wound healing.

Materials and Methods

Materials

Rhizomes of *C. longa*, leaves of *M. citrifolia*, whole plant of *T. procumbens*, and leaves of *L. camara* were sourced from the herbal garden and premises of Sri Adichunchanagiri College of Pharmacy, B G Nagara. Silver nitrate was purchased from Lobie Chemie Pvt. Ltd., Poloxamer 407 was purchased from Indian Fine Chemicals. DPPH from Sigma-Aldrich, phenol reagent from HiMedia, and C2C12 murine myoblast cell lines were procured from Adichunchanagiri Institute of Molecular Medicine, B G Nagara.

Selection and Preparation of Plant Extracts and Phytochemical Profiling

The extraction process was carried out using a modified steam distillation process, as shown in Figure 1(a). Fresh rhizomes of *C. longa*, leaves of *M. citrifolia* and *L. camara* and a whole *T. procumbens* plant were collected from Sri Adichunchanagiri College of Pharmacy, B G Nagara. The collected plant parts were washed thoroughly and shade-dried to remove any impurities. 100 g of plant material was weighed accurately and subjected to steam distillation using a steam distillation apparatus until the same quantity of hydrosol was obtained. The plant material was then removed and cut into smaller fragments for further extraction using the maceration technique of water as a solvent for 21 days, using a sterile sealed container to avoid contamination. The final aqueous extract solution was then filtered thoroughly using Whatman filter paper. The final extracts of *C. longa, M. citrifolia, L. camara* and *T. procumbens* were mixed uniformly in the ratio of 3:2:1:1 based on their antioxidant activity and wound healing potential.

Formulation of Polyherbal Silver Nanoparticles

The final polyherbal formulation was used to formulate the AgNPs as per the green synthesis method (Ravindran et al., 2019). 17 mg of silver nitrate was weighed accurately and dissolved in 100 mL of Millipore water to form a 0.1 mM silver nitrate solution. The formulation was carried out using the green synthesis method of AgNP synthesis. 5 and 10 mL of extracts were added dropwise to 95 and 90 mL of 0.1 mM silver nitrate solution, respectively, to form two separate formulations. The mixture was stirred for 8 h using a magnetic stirrer. After stirring, the resultant solution was kept in a dark place for 24 h to allow the formation of polyherbal AgNPs. The solution was then subjected to centrifugation at 7,500 rpm for 30 min. The supernatant was discarded, and the AgNPs at the bottom were collected and washed using methanol multiple times, as shown in Figure 1(b).

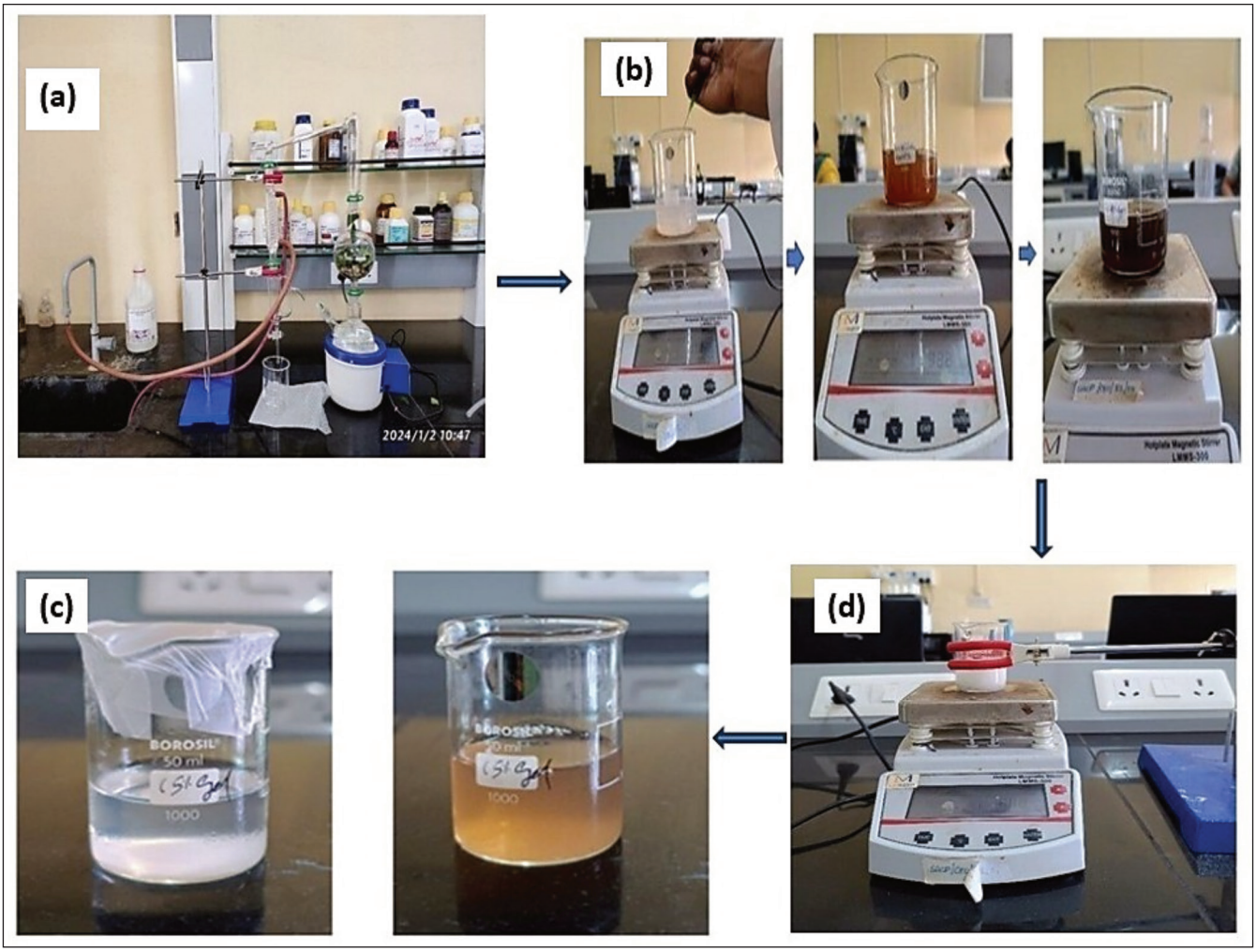


Figure 1. (a) Extraction of Phytoconstituents Using Modified Steam Distillation Method. (b) Formulation of Polyherbal Silver Nanoparticles. (c) Formulation of Silver Nanoparticle (AgNP)-loaded Thermoreversible Poloxamer 407 Gel. (d) 5% PH-Silver Nanoparticles (AgNP)-loaded Gel (b) 5% PH-extract Loaded Gel.

Formulation of Polyherbal Silver Nanoparticle-loaded Topical Gel

The formed polyherbal AgNP gel was formulated into a topical gel using Poloxamer 407 using the cold method (Chinnasamy et al., 2021). Poloxamer 407 gel was prepared by using 0.2% AgNPs (w/w). 100 mL of Millipore water was autoclaved to remove bacterial impurities and refrigerated for 4 h. This ice-cold water was taken, and 20 g of Poloxamer 407 was added slowly until completely dissolved using a magnetic stirrer, as shown in Figure 1(c) and 1(d). Poloxamer 407 was used as the gelling agent due to the property of thermoreversible gelation, that is, the formulation exhibits the property of a solution nature at temperatures below physiological conditions and, on heating, forms a gel at physiological temperatures. This property adds to the ease of use and will help the formulation stick to the wound site once it comes in contact with it. Moreover, since it is already established as biocompatible with low toxicity, it is an ideal choice for topical biomedical usage. More noteworthy, it has been highly reported that Poloxamer 407 increases the sustained release of lyophilized nanoparticles and drugs, thus extending the therapeutic effect of drugs at the target site. All these characteristics were reasons to justify its application in our polyherbal gel-loaded AgNP formulation. The entire formulation process was conducted sterilely using a sterilized laminar airflow to prevent bacterial contamination. After the complete dissolution of the polymer, the solution was kept in a refrigerator for 24 h to ensure complete dissolution. The solutions were taken out after 24 h and allowed to gel at room temperature.

Evaluation of Topical Gel

Physical Appearance

The gel formulations were visually evaluated for their appearance, consistency, presence of bubbles, and color.

Spreadability

1 g of formulated gel was placed at the center of a glass plate, upon which another glass plate was placed. A 100 g standard weight was placed upon the glass plates to ensure the gel spreads across the plates. The weight was taken out after 10 min, and the spreadability was measured using a digital vernier caliper. The study was done in triplicate, and the final values were measured as the mean and standard deviation.

pH

A 1% solution of all the prepared gel formulations in distilled water was made and stirred using a magnetic stirrer for 1 h. After that, pH measurement was done using a digital pH meter (Alfaris et al., 2022).

Viscosity

The viscosity of formulated gels was evaluated using a Brookfield viscometer using spindle number 06 at 50 rpm at room temperature (Garala et al., 2013).

Total Phenolic Content

The total phenolic content of the polyherbal extract was determined by the Folin–Ciocalteau method. In this procedure, various concentrations of the sample ranging from 10 to 100 µL were taken and diluted with methanol, making it up to 400 µL. 2 mL of phenol reagent was added to this mixture along with 1.6 mL of sodium carbonate (7.5%w/v). This solution was vortexed thoroughly and incubated for 60 min in dark conditions. The absorbance was measured using a UV spectrophotometer at 715 nm. Gallic acid was used as a standard, and a calibration curve was plotted. The results were depicted in terms of gallic acid equivalent per gram of dry weight (Dhiraj Kamath et al., 2015).

In Vitro Antioxidant Activity

4 mg of DPPH was dissolved in 100 mL of methanol to form a 0.1 mM DPPH stock solution. Polyherbal extracts ranging from 10 to 100 µL were added to the DPPH solution to make it up to 1 mL. The mixture was further diluted by adding 1 mL of methanol and incubated at room temperature for 30 min after mixing the solution by vortexing it thoroughly. The mixture was analyzed spectrophotometrically using a UV spectrophotometer at 517 nm, and the absorbance was recorded. The scavenging activity will be calculated as the percentage of DPPH radical scavenged using the formula (Kumar & Ojha, 2014):

$$\% \text{ Radical Scavenging Activity} = \text{Absorbance (control)} - \text{Absorbance (sample)}/\text{Absorbance (control)} \times 100$$

In Vitro Wound Healing Assay

An *in vitro* wound healing assay was performed using C2C12 murine myoblast cell lines as per the procedure (Hour et al., 2022). C2C12 cells were seeded in a 12-well dish and allowed to attach overnight in 800 µL DMEM medium (per well). A scratch was made using a sterilized microtip, and the scar was imaged and treated with AgNP-loaded gel and polyherbal extract-loaded gels, and allowed to incubate. Imaging was done at different intervals at 6 and 12 h, using an Olympus microscope. The migration of myoblast cells into the scratched area was observed and analyzed using ImageJ software.

In Vivo Wound Healing Using the Excision Wound Model

Animal experiments were carried out with the approval of the Institutional Animal Ethical Committee (IAEC), Sri Adichunchanagiri College of Pharmacy, B G Nagara (Approval Number: SACCP-IAEC/2024-01/106). A total of 36 male Wistar albino rats were chosen for the animal experiment, which were divided into six groups containing six rats in each group. Pathogen-free, healthy rats with body weights around 180–200 g were maintained in standard laboratory conditions with a 12-h day and 12-h night cycles. Animals were fed a standard rodent diet and purified RO water throughout the experiment. After 7 days of acclimatization, rats were anesthetized using diethyl ether. Dorsal skin was shaved and disinfected with ethanol (70% v/v).

1. Group I: Control
2. Group II: Standard (Silverex gel)
3. Group III: 5% polyherbal extract-loaded gel
4. Group IV: 10% polyherbal extract-loaded gel
5. Group V: 5% polyherbal AgNP-loaded gel
6. Group VI: 10% polyherbal AgNP-loaded gel

A 6 mm mechanical biopsy punch was used for inducing wounds on the dorsal surface, and a sterilized surgical blade was used to remove the excess skin after punching. An equal amount of gel was smeared on the wound surface, and wounds were covered with a transparent dressing material. Wound areas were examined on the 1st, 3rd, 5th, 7th, 9th, 12th, and 15th days and were measured using digital Vernier calipers to record the decrease in wound area. No signs of irritation, infection, or mortality were observed in any of the treatment groups during the course of the animal studies, confirming the tolerability of the formulations. The percentage of wound contraction was calculated using the following formula:

$$\text{Percentage of Wound contraction} = (\text{Wound area on day 1} - \text{Wound area on day '}n\text{'})/\text{Wound area on day 1} \times 100$$

Statistical Analysis

The statistical analysis of the animal study was performed using one-way analysis of variance (ANOVA) using GraphPad Prism 8.0 software. The mean results of the formulations were compared to those of the control group.

Results

Preliminary Phytochemical Analysis

Preliminary phytochemical analysis was carried out using a standardized phytochemical screening procedure. The detailed results of the phytochemical screening are presented in Table 1 (Soni & Sosa, 2013).

Evaluation of Polyherbal Silver Nanoparticles

UV–Visible Spectrophotometric Evaluation

The AgNPs were prepared using the green synthesis method, and a Shimadzu UV–visible spectrophotometer was used to measure the particles. A spectrum was scanned from 200 to 800 nm using water as a blank. The peak, which showed the production of AgNPs, was seen at 420 and 421 nm (Agustina et al., 2021). The spectrum was obtained at several intervals, including day 1, 5, 7, 15, and 30, in order to verify the stability of the polyherbal AgNPs that were created. Because of the surface plasmon phenomenon, AgNPs are known to create a UV spectrum peak between 400 and 500 nm (Ashraf et al., 2016). The formed nanoparticles also exhibit the same behavior, indicating the formation of AgNPs as shown in Figure 2(a).

Fourier Transform Infrared Spectroscopy

To find out if polyherbal AgNPs were present, a Fourier transform infrared (FTIR) analysis of AgNPs was carried out. The FTIR study results revealed three distinct bond lengths at distinct peaks: the 1741–C=O stretch, the 1303–C–O aliphatic stretch, and the 1181–C–H aliphatic stretch. AgNPs' FTIR spectra showed notable peaks at 1,303.92, 1,708, and 2,725.1 cm^{-1}, in that order, as shown in Figure 2(b).

Table 1. Preliminary Phytochemical Analysis of Polyherbal Extract.

Sl. No.	Phytoconstituents	*Curcuma longa*	*Morinda citrifolia*	*Tridax procumbens*	*Lantana camara*	Polyherbal Extract
1	Alkaloids	+	–	+	+	+
2	Glycosides	+	+	–	+	+
3	Saponins	+	+	+	+	+
4	Tannins	+	+	+	–	+
5	Phenolic compounds	+	+	+	+	+
6	Flavonoids	+	+	+	–	+
7	Steroids	+	+	+	+	+
8	Volatile oils	+	+	+	+	+

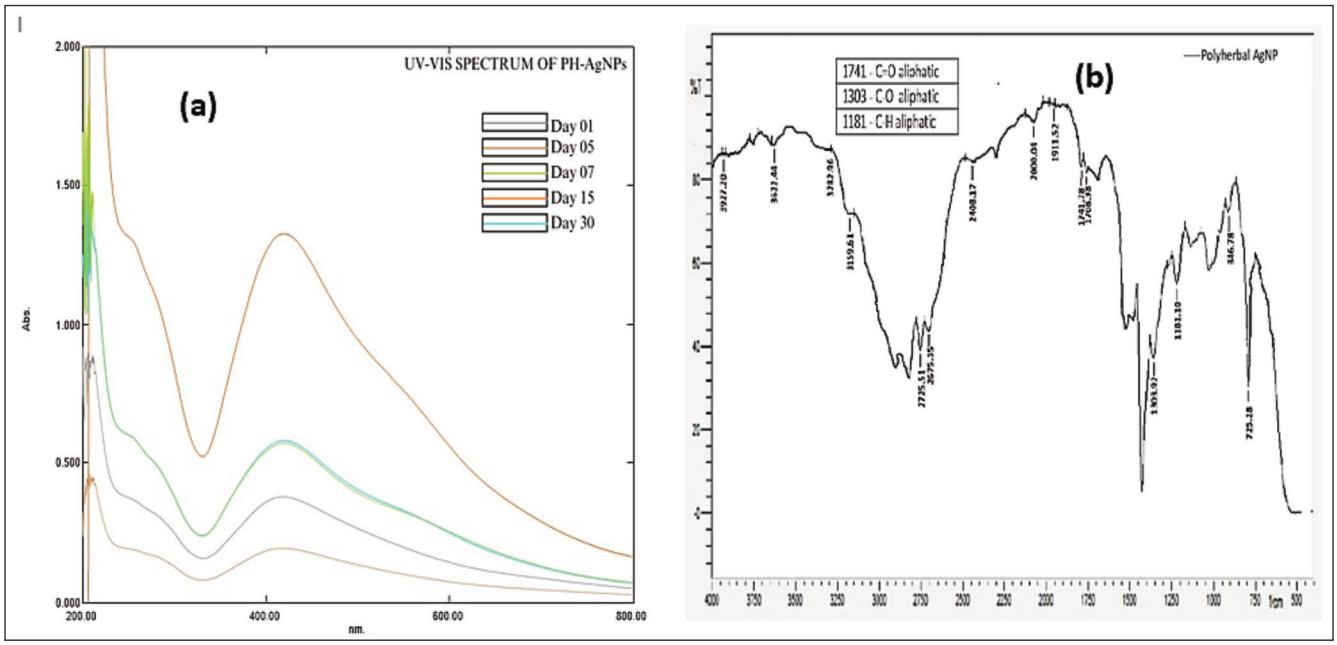


Figure 2. (a) UV–Visible Spectrum of Polyherbal Silver Nanoparticles at Different Time Intervals. (b) Fourier Transform Infrared (FTIR) Spectrum of Polyherbal Silver Nanoparticles (AgNPs).

Particle Size, Zeta Potential, and Polydispersity Index

The Anton Paar Litesizer-500 was used to measure the produced AgNPs' particle size. The polydispersity index, zeta potential, and particle size of the two AgNP formulations, 5% and 10% polyherbal AgNPs, were examined. The polydispersity index of 10% and 5% of polyherbal AgNPs, respectively, was 0.262 ± 0.014 nm and 111.27 ± 3.36 nm, respectively, whereas the polydispersity index of 5% of polyherbal AgNPs was 234.26 ± 20.27 nm. It was discovered that 10% PH AgNPs had a zeta potential of −11.13 ± 0.8 mV. 5% polyherbal nanoparticles were discovered to have a zeta potential of −15.87 ± 4.66 mV, as shown in Figure 3(a) and 3(b).

Evaluation of Antioxidant Activity Using DPPH Radical Scavenging Assay

The DPPH assay was used to assess the antioxidant activity of the plant extracts, and the findings are displayed in the table. At a higher concentration, the polyherbal mixture

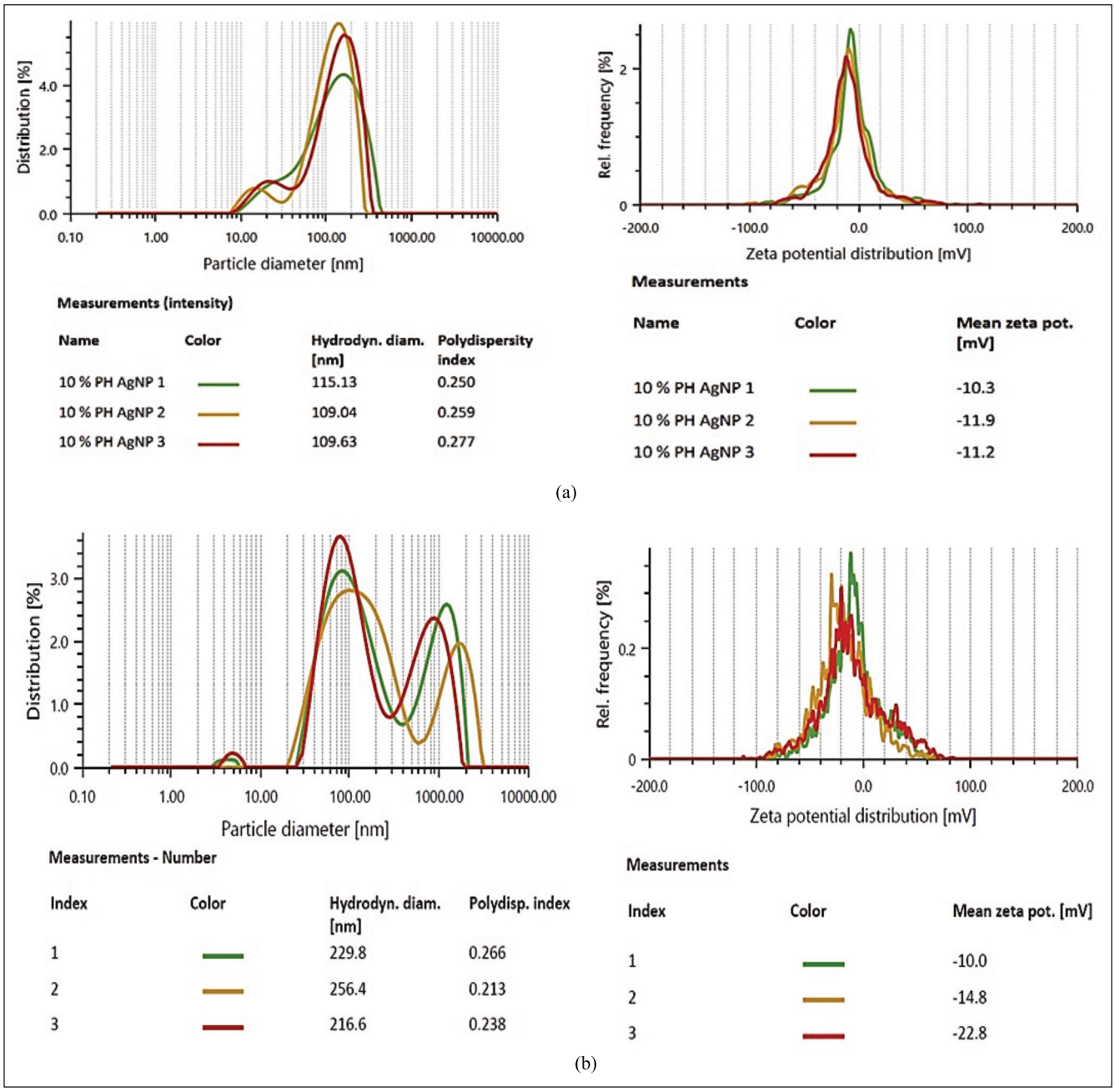


Figure 3. (a) Particle Size and Zeta Potential of 10% PH-Silver Nanoparticles (AgNPs). (b) Particle Size and Zeta Potential of 5% PH-Silver Nanoparticles (AgNPs).

exhibits synergistic activity with 84.71% ± 0.91% of inhibition. The antioxidant activity of individual plants such as *C. longa, M. citrifolia, T. procumbens*, and *L. camara* show a percentage inhibition of 81.25% ±5.21%, 75.94% ± 4.33%, 66.09% ± 2.16%, and 69.73% ± 1.23% at a higher concentration, as presented in Table 2.

Total Phenolic Content Using the Folin–Ciocalteau Method

The plant extracts were evaluated for their total phenolic content using the Folin–Ciocalteau assay method. Gallic acid was used as a standard, and the plant extracts were estimated spectrophotometrically at 765 nm. The standard curve for gallic acid was plotted at different concentrations, and the equation and regression factor were calculated.

Phenolic compounds are important in plants for their redox properties. As presented in Table 3, the phenolic content of the plants is measured to facilitate free radical scavenging. The results were derived from the calibration curve and expressed in the gallic acid equivalent per gram of the phenolic content of *C. longa, M. citrifolia, T. procumbens*, and *L. camara* (64.96 ± 1.42, 75.27 ± 1.06, 39.98 ± 0.29, 59.40 ± 5.74). The polyherbal mixture shows a 94.83 ± 0.79 of phenolic content expressed in terms of gallic acid equivalent per gram in dry weight.

Evaluation of Topical Gel

Physical Appearance

The physical appearance of the prepared gels against lighter and darker backgrounds was assessed. In contrast to the AgNP-loaded gels, which displayed a clear white gel, the herbal extract-loaded gels maintained the color of the extracts, giving them a pale yellow to yellowish color.

Spreadability

By placing 1 g of gel between two glass plates and applying 100 g of weight for a brief period, the spreadability of the gel was determined. A computerized vernier caliper was used to measure the extent of the gel distribution. The investigation was carried out in triplicate, and the values in Table 4 were shown as mean and standard deviation.

pH

pH was measured using a digital pH meter (LabIndia) in triplicate, and pH was expressed in terms of mean and standard deviation (Table 4).

Table 2. Percentage of DPPH at Different Concentrations.

Sl. No.	Concentration (µg/mL)	Percentage of Inhibition (in %)				
		Curcuma longa	*Morinda citrifolia*	*Tridax procumbens*	*Lantana camara*	Polyherbal Mixture
1	0	0	0	0	0	0
2	10	9.58 ± 3.78	13.6 ± 1.11	20.69 ± 1.30	3.45 ± 2.18	49.43 ± 1.10
3	20	24.14 ± 1.22	11.11 ± 3.24	44.83 ± 2.80	8.43 ± 3.12	49.62 ± 0.87
4	30	24.52 ± 3.00	17.43 ± 5.64	61.49 ± 3.11	17.05 ± 4.11	49.81 ± 0.69
5	40	26.44 ± 4.11	20.11 ± 1.36	71.46 ± 4.65	17.24 ± 5.63	50.38 ± 0.63
6	50	34.86 ± 1.25	24.71 ± 4.21	73.95 ± 3.87	22.03 ± 6.34	51.53 ± 1.23
7	60	41.67 ± 2.14	33.72 ± 6.38	71.07 ± 6.34	30.65 ± 5.51	58.21 ± 1.36
8	70	49.08 ± 2.45	48.47 ± 4.69	70.69 ± 7.11	44.06 ± 4.11	67.92 ± 0.74
9	80	51.38 ± 3.33	51.92 ± 4.87	49.04 ± 3.10	56.7 ± 3.87	73.84 ± 0.25
10	90	63.02 ± 4.11	57.41 ± 3.11	56.86 ± 2.11	57.66 ± 6.97	79.84 ± 0.67
11	100	71.25 ± 5.21	68.94 ± 4.33	66.09 ± 2.16	64.73 ± 1.23	84.71 ± 0.91

Table 3. Total Phenolic Content (GAE/g of Dry Weight) of Herbal Extracts.

Sl. No.	Plant Extracts	GAE/g of Dry Weight
1	*Curcuma longa*	64.96 ± 1.42
2	*Morinda citrifolia*	75.27 ± 1.06
3	*Tridax procumbens*	39.98 ± 0.29
4	*Lantana camara*	59.40 ± 5.74
5	Polyherbal mixture	94.83 ± 0.79

Viscosity

The viscosity of the gel formulations was calculated at room temperature using a Brookfield viscometer with a spindle number 6. The viscosity of the formulations ranged from 12,700 to 14,500 cP. Measurements were taken in triplicate and expressed in centipoise with mean and standard deviation in Table 4.

In Vitro Wound Healing Assay

For the *in vitro* wound healing experiment, C2C12 murine myoblast cell lines were used. To measure the migration of myoblast cells into the wound area, imaging was performed at 6 and 12 h using the cell scratch test method, as shown in Figure 4(a). The 10% AgNP-loaded gel formulation was shown to have helped with wound closure out of the four formulations and to have the greatest myoblast migration into the wound area.

In Vivo Wound Healing Assay

The progress of each animal group's wound healing is shown in Figure 4(b). Group IV, the animals treated with 10% polyherbal AgNP-loaded gel, had a wound healing percentage of 95.18%, which is a significantly greater rate of wound recovery. Figure 4(b) displays the proportion of each group's wound healing. When compared to raw extract-laden gel, the groups loaded with polyherbal nanoparticle gel demonstrated superior rates of wound healing and tissue regeneration. The standard group demonstrated 67.78% wound healing, 5% polyherbal extract-loaded gel demonstrated 65.04%, 10% polyherbal gel-loaded gel demonstrated 83.15%, and 5% polyherbal AgNP-loaded gel demonstrated 93.51% wound healing when compared to the control group's 38.87% wound healing percentage as presented in Table 5. The AgNP-loaded gel showed better tissue regeneration than extract-loaded gels and control groups.

The 10% polyherbal nanoparticle cell was also subjected to a cytotoxicity study on the C2C12 cell lines to analyze the impact of the gel formulations on the murine myoblast cells. The gel formulations showed no signs. The higher efficiency of wound healing rates revealed in the case involving the polyherbal AgNP-loaded gel is most probably the result of a combination effect rather than of a specific pharmacological effect. The antioxidant capacity, which is backed up with the presence of phenolic compounds and further confirmed with the DPPH radical scavenging activity, is one that counteracts

Table 4. Evaluation of Gel Formulations.

Sl No.	Formulation	Appearance	pH	Spreadability (in cm)	Viscosity (in cP)
1	5% PH gel	Pale yellow	6.02 ± 0.06	3.53 ± 0.57	13,628 ± 1.22
2	10% PH gel	Yellow	6.08 ± 0.08	4.35 ± 0.64	13,831 ± 2.66
3	5% PH-AgNP gel	Clear white	5.87 ± 0.05	4.89 ± 0.22	12,725 ± 0.77
4	10% PH-AgNP gel	Clear white	5.93 ± 0.03	5.59 ± 0.55	14,520 ± 0.69

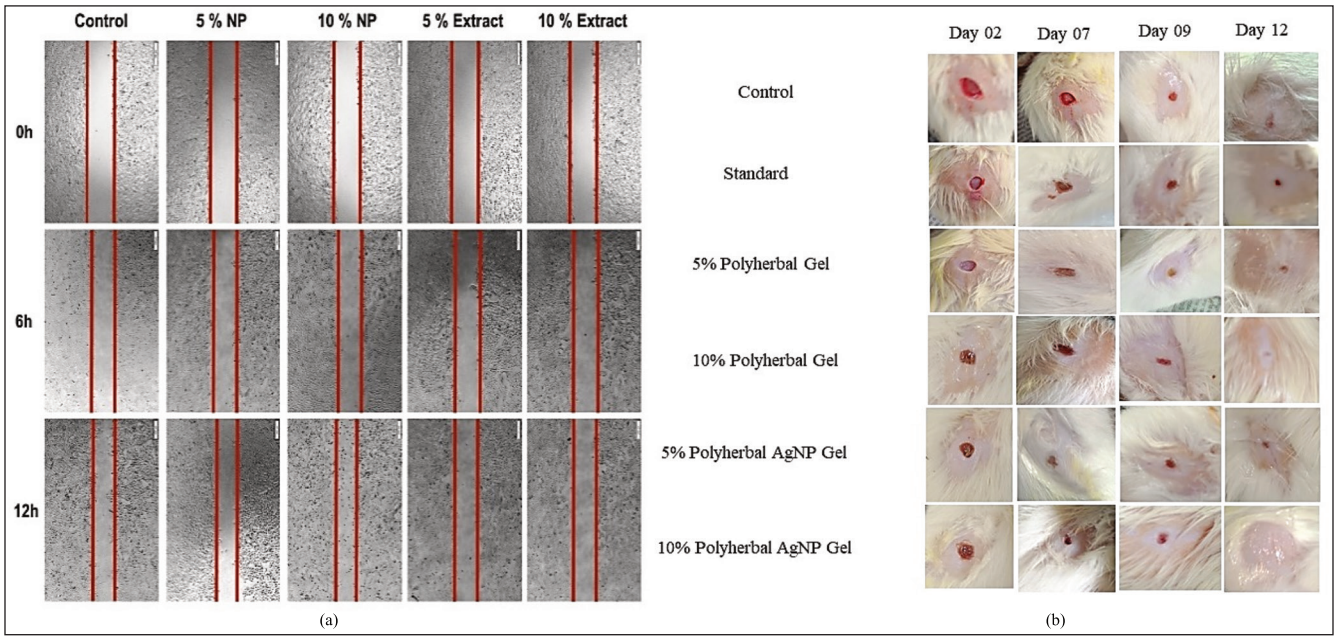


Figure 4. (a) *In Vitro* Wound Healing Using the Cell Scratch Assay. (b) *In Vivo* Wound Healing in Animal Groups.

Table 5. Wound Contraction Rate at Different Intervals (in %).

Wound Contraction (in %)	Groups of Animals						
	Time Interval (in days)	**Control**	**Standard**	**5% PH Gel**	**10% PH Gel**	**5% PH AgNP Gel**	**10% PH AgNP Gel**
	Day 1	0.00	0.00	0.00	0.00	0.00	0.00
	Day 3	1.72	14.51	8.46	16.54	7.70	15.09
	Day 5	12.85	32.22	20.16	33.23	29.40	31.30
	Day 7	21.47	39.87	33.01	48.52	51.26	59.87
	Day 12	36.99	62.52	50.89	60.53	74.06	83.15
	Day 15	38.87	67.78	65.04	83.15	91.51	95.18

the effect of oxidative stress that is posed at the wound site. Simultaneously, the anti-microbial potential of both AgNPs and the phytochemicals in the herbal extracts will aid in the reduction of the load of microorganisms, thus preventing infection and aiding faster tissue repair. Besides, the bioactive constituents have anti-inflammatory activities and help regulate the inflammatory stage of wound healing. Collectively, these synergistic antioxidant, anti-microbial, and anti-inflammatory effects yield a multi-dimensional rationale for the enhanced wound closure rate *in vivo* of cytotoxicity until the concentration of 200 μg/mL per well. The superior performance of the 10% PH-AgNP gel can be attributed to a synergistic mechanism wherein AgNPs exert broad-spectrum anti-microbial activity, modulate pro-inflammatory mediators (e.g., TNF-α, IL-1β), and stimulate angiogenesis. Concurrently, herbal bioactives—including curcuminoids (*C. longa*), iridoid glycosides (*M. citrifolia*), flavonoids (*T. procumbens*), and phenolic terpenoids (*L. camara*)—provide potent antioxidant effects, inhibit excessive inflammation, promote fibroblast proliferation, and enhance collagen synthesis. This dual action reduces infection risk, limits oxidative stress, and accelerates tissue repair and remodeling, consistent with previous reports on combined herbal-nanoparticle systems.

The higher efficiency of wound healing rates revealed in the case involving the polyherbal AgNP-loaded gel is most probably the result of a combination effect rather than of a specific pharmacological effect. The antioxidant capacity, which is backed up with the presence of phenolic compounds and further confirmed with the DPPH radical scavenging activity, is one that counteracts the effect of oxidative stress that is posed at the wound site. Simultaneously, the anti-microbial potential of both AgNPs and the phytochemicals in the herbal extracts will aid in the reduction of the load of microorganisms, thus preventing infection and aiding faster tissue repair. Besides, the bioactive constituents have anti-inflammatory activities and help regulate the inflammatory stage of wound healing. Collectively, these synergistic antioxidant, anti-microbial, and anti-inflammatory effects yield a multi-dimensional rationale for the enhanced wound closure rate *in vivo*.

Statistical Analysis

The concentration-dependent inhibitory activity of *C. longa, M. citrifolia, T. procumbens, L. camara*, and the polyherbal mixture is illustrated in Figure 5(a), and the percentage of wound healing over different days is shown in Figure 5(b). To identify which specific groups differed, a *post hoc* Tukey's honestly significant difference (HSD) test was performed. The results showed the following:

- 5% AgNP gel and 10% AgNP gel demonstrated the highest mean percentages of wound contraction at day 15, with values of 91.51% and 95.18%, respectively.
- The 10% PH gel also showed significant improvement, with a mean contraction of 83.15%.
- The standard treatment and 5% PH gel had moderate effects, with mean contractions of 67.78% and 65.04%, respectively.
- The control group had the lowest mean contraction percentage at day 15, at 38.87%.

With a considerable advantage over all other groups, the 10% AgNP gel was found to be the most effective treatment for improving wound contraction, according to the one-way ANOVA and *post hoc* analysis that followed. The results imply that AgNP-containing formulations can significantly enhance wound healing results. The possible utility of AgNP gels in clinical wound care applications is supported by these findings. The underlying processes and long-term impacts of these interventions on wound healing may be investigated in further research.

Significant variations in wound diameters between the treatment groups and the control group were found using a one-way ANOVA and Dunnett's *post hoc* test ($p < .05$). The gel loaded with 5% polyherbal PH AgNP and the gel containing 10% PH AgNP were found to be the most effective in healing wounds, as seen by the significantly decreased mean wound size compared to the control group.

Discussion

The present study demonstrates the successful formulation of a polyherbal AgNP-loaded thermosensitive gel and its

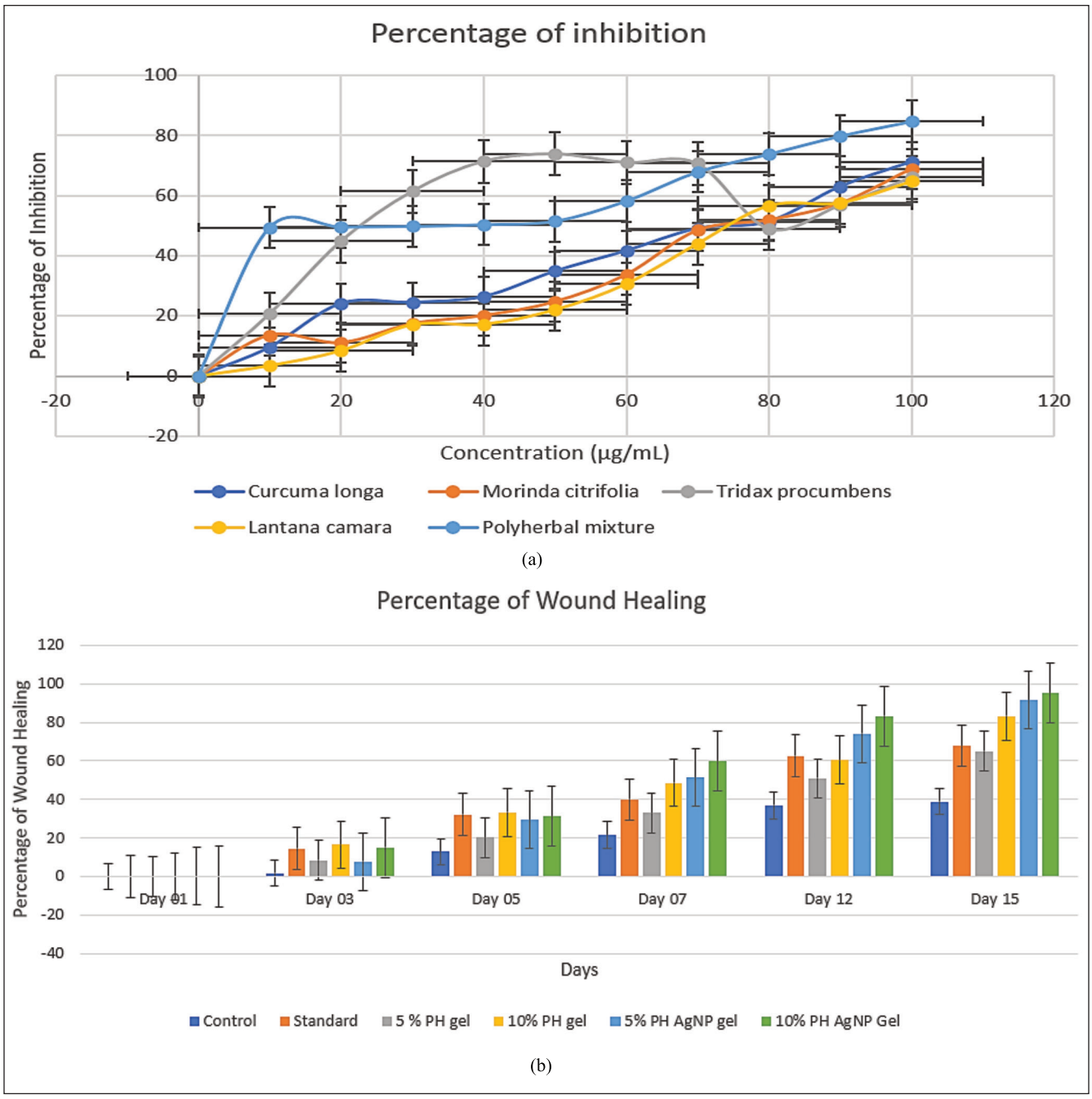


Figure 5. (a) Percentage of Inhibition. (b) Percentage of Wound Healing Across Different Time Intervals.

significant efficacy in promoting acute wound healing. Green synthesis using combined extracts of *C. longa, M. citrifolia, T. procumbens*, and *L. camara* produced stable AgNPs, as confirmed by UV–visible spectroscopy and FTIR analysis, with characteristic surface plasmon resonance around 420 nm, consistent with earlier reports on plant-mediated AgNP synthesis (Agustina et al., 2021; Ashraf et al., 2016). The optimized formulation exhibited a nanoscale particle size (111.27 ± 3.36 nm) and moderately negative zeta potential (−11.13 ± 0.8 mV), indicating suitability for topical application. Incorporation of these AgNPs into a Poloxamer 407-based thermosensitive gel yielded formulations with acceptable pH, viscosity, and spreadability, supporting their dermal compatibility and ease of application (Garala et al., 2013; Russo & Villa, 2019).

Oxidative stress is a major impediment to wound repair, as excessive reactive oxygen species can damage cellular structures and prolong inflammation (Rodrigues et al., 2019; Wilkinson & Hardman, 2020). In this study, the polyherbal extract exhibited significantly higher antioxidant activity

than individual plant extracts, demonstrated by strong DPPH radical scavenging (84.71% ± 0.91%) and elevated total phenolic content (94.83 ± 0.79 mg GAE/g). Phenolic compounds and flavonoids are known to protect fibroblasts and keratinocytes from oxidative injury, thereby facilitating faster granulation and epithelialization (Sharma et al., 2021; Soni & Sosa, 2013). The synergistic antioxidant effect observed here likely arises from the complementary phytochemical profiles of the selected plants, each previously reported to possess wound-healing and free radical scavenging properties (Irham & Hardiyanti, 2021; Jyotirmayee & Mahalik, 2022; Yaduvanshi et al., 2011).

Beyond antioxidant activity, effective wound healing requires control of microbial load and appropriate modulation of inflammation. AgNPs are well established as broad-spectrum anti-microbial agents, acting through membrane disruption, oxidative damage, and inhibition of microbial replication (Ashraf et al., 2016; Chinnasamy et al., 2021). The incorporation of AgNPs into the polyherbal gel likely reduced infection risk at the wound site, contributing to the superior healing outcomes observed *in vivo*. In parallel, phytoconstituents such as curcuminoids, iridoid glycosides, and flavonoids are known to downregulate pro-inflammatory mediators including TNF-α, IL-1β, and nitric oxide, thereby preventing prolonged inflammation and enabling timely progression to the proliferative phase (Coutinho de Sousa et al., 2017; Irham & Hardiyanti, 2021). The nanoscale delivery of these bioactives may further enhance their local bioavailability, resulting in synergistic anti-microbial and anti-inflammatory effects consistent with earlier reports on herbal-nanoparticle hybrid wound therapies (Fatima et al., 2021; Ravindran et al., 2019).

The choice of Poloxamer 407 as the delivery matrix further strengthens the therapeutic potential of the formulation. Its thermoreversible sol–gel transition allows convenient application in liquid form followed by rapid gelation at physiological temperature, ensuring prolonged retention at the wound site (Russo & Villa, 2019). Such sustained contact facilitates controlled release of AgNPs and phytochemicals, improving local efficacy compared with conventional extract-loaded gels that may suffer from poor retention or rapid degradation. The superior wound contraction achieved with the 10% polyherbal AgNP gel aligns with previous studies reporting enhanced epithelialization, collagen deposition, and angiogenesis using nanoparticle-loaded hydrogel systems (Chinnasamy et al., 2021; Sharma et al., 2021).

Notwithstanding these promising findings, certain limitations warrant consideration. The absence of histopathological analysis restricts direct assessment of tissue remodeling processes such as collagen organization, angiogenesis, and inflammatory cell infiltration (Kordestani, 2019). While cytotoxicity studies confirmed safety up to 200 μg/mL in C2C12 cells, further evaluation using human skin-relevant cell lines and long-term exposure models is required. Additionally, stability, scalability, and regulatory considerations related to nanoparticle-based formulations must be addressed prior to clinical translation. Future investigations should incorporate histological and molecular analyses, assess efficacy in chronic or infected wound models, and explore large-scale manufacturing feasibility to support clinical development.

Conclusion

This study developed and evaluated a novel wound healing gel integrating traditional herbal medicine with nanotechnology and thermosensitive materials. The extract of the *C. longa, M. citrifolia, T. procumbens*, and *L. camara* in the polyherbal AgNP gel (10%) showed excellent wound healing potential (95.18% healing) in animal models. Although these results are encouraging regarding acute wound treatment, the associated limitations include stability and scalability, sustainability, clinical translation, among others and with success, these aspects still have to be addressed in future studies before their potential application to clinics. To increase its generalizability, it will be important to pursue in the future (a) formulation optimization and stability testing, (b) more comprehensive toxicological studies, (c) *in vitro* work on skin-relevant human cell lines, and (d) explorations of translation pathways to the clinic.

Acknowledgments

The authors acknowledge King Faisal University, Al-Ahsa, Saudi Arabia and Sri Adichunchanagiri College of Pharmacy, Karnataka, India, for providing support to carry out the present work.

Declaration of Conflicting Interests

The authors declared no potential conflicts of interest with respect to the research, authorship, and/or publication of this article.

Ethical Approval and Informed Consent

Animal experiments were carried out with the approval of the Institutional Animal Ethical Committee (IAEC), Sri Adichunchanagiri College of Pharmacy, B G Nagara (Approval Number: SACCP-IAEC/2024-01/106).

Funding

The authors disclosed receipt of the following financial support for the research, authorship, and/or publication of this article: This work was supported by the Deanship of Scientific Research, Vice Presidency for Graduate Studies and Scientific Research, King Faisal University, Saudi Arabia (Grant No. KFU253301).

ORCID iD

Vedamurthy Joshi https://orcid.org/0000-0001-7732-3842

References

Agustina, T. E., Handayani, W., & Imawan, C. (2021). The UV-vis spectrum analysis from silver nanoparticles synthesized using *Diospyros maritima* Blume leaves extract. In *Proceedings of the*

3rd KOBI Congress, International and National Conferences (KOBICINC 2020) (pp. 411–419). Atlantis Press. https://doi.org/10.2991/absr.k.210621.070

Alfaris, S. M., Dhahir, R. K., & Al-Nima, A. M. (2022). Preparation and evaluation of propolis extract gel and exploration of its antioxidant and antimicrobial activity. *Pharmacognosy Journal*, *14*(6), 675–681. https://doi.org/10.5530/pj.2022.14.153

Ashraf, J. M., Ansari, M. A., Khan, H. M., Alzohairy, M. A., & Choi, I. (2016). Green synthesis of silver nanoparticles and characterization of their inhibitory effects on AGEs formation using biophysical techniques. *Scientific Reports*, *6*, 20414. https://doi.org/10.1038/srep20414

Chinnasamy, G., Chandrasekharan, S., Koh, T. W., & Bhatnagar, S. (2021). Synthesis, characterization, antibacterial and wound healing efficacy of silver nanoparticles from *Azadirachta indica*. *Frontiers in Microbiology*, *12*, 611560. https://doi.org/10.3389/fmicb.2021.611560

Coutinho de Sousa, B., Reis Machado, J., da Silva, M. V., da Costa, T. A., Lazo-Chica, J. E., Degasperi, T. P., Rodrigues Junior, V., Sales-Campos, H., Uber Bucek, E., & Freire Oliveira, C. J. (2017). *Morinda citrifolia* (noni) fruit juice reduces inflammatory cytokine expression and contributes to the maintenance of intestinal mucosal integrity in DSS experimental colitis. *Mediators of Inflammation*, *2017*, 6567432. https://doi.org/10.1155/2017/6567432

Dhiraj Kamath, S., Arunkumar, D., Avinash, N. G., & Samshuddin, S. (2015). Determination of total phenolic content and total antioxidant activity in locally consumed foodstuffs in Moodbidri, Karnataka, India. *Advances in Applied Science Research*, *6*(6), 99–102.

Fatima, F., Aldawsari, M. F., Ahmed, M. M., Anwer, M. K., Naz, M., Ansari, M. J., Hamad, A. M., Zafar, A., & Jafar, M. (2021). Green synthesized silver nanoparticles using *Tridax procumbens* for topical application: Excision wound model and histopathological studies. *Pharmaceutics*, *13*(11), 1754. https://doi.org/10.3390/pharmaceutics13111754

Garala, K., Joshi, P., Patel, J., Ramkishan, A., & Shah, M. (2013). Formulation and evaluation of periodontal *in situ* gel. *International Journal of Pharmaceutical Investigation*, *3*(1), 29–41. https://doi.org/10.4103/2230-973X.108961

Hour, T. C., Vo, T. C. T., Chuu, C. P., Chang, H. W., Su, Y. F., Chen, C. H., & Chen, Y. K. (2022). The promotion of migration and myogenic differentiation in skeletal muscle cells by quercetin and underlying mechanisms. *Nutrients*, *14*(19), 4106. https://doi.org/10.3390/nu14194106

Irham, W. H., & Hardiyanti, R. (2021). Wound healing bioactivity of *Curcuma longa* Linn. *Rasayan Journal of Chemistry*, *14*(4), 2386–2391. https://doi.org/10.31788/RJC.2021.1446345

Jyotirmayee, B., & Mahalik, G. (2022). A review on selected pharmacological activities of *Curcuma longa* L. *International Journal of Food Properties*, *25*(1), 1377–1398. https://doi.org/10.1080/10942912.2022.2082464

Kordestani, S. S. (2019). *Atlas of wound healing: A tissue regeneration approach*. Academic Press.

Kumar, B., Vijayakumar, M., Govindarajan, R., & Pushpangadan, P. (2007). Ethnopharmacological approaches to wound healing—Exploring medicinal plants of India. *Journal of Ethnopharmacology*, *114*(2), 103–113. https://doi.org/10.1016/j.jep.2007.08.010

Kumar, S., & Ojha, S. (2014). Evaluation of antioxidant activity and total phenol content in different varieties of *Lantana camara* leaves. *BMC Research Notes*, *7*, 560. https://doi.org/10.1186/1756-0500-7-560

Raghupathy, S., Vaidyanathan, L., & Sivaswamy, L. T. S. (2017). Adult zebrafish model of wound inflammation to study wound healing potency of *Curcuma longa* extracts. *Annual Research & Review in Biology*, *18*(3), 1–8. https://doi.org/10.9734/ARRB/2017/35910

Ravindran, J., Arumugasamy, V., & Baskaran, A. (2019). Wound healing effect of silver nanoparticles from *Tridax procumbens* leaf extracts on *Pangasius hypophthalmus*. *Wound Medicine*, *27*, 100170. https://doi.org/10.1016/j.wndm.2019.100170

Rodrigues, M., Kosaric, N., Bonham, C. A., & Gurtner, G. C. (2019). Wound healing: A cellular perspective. *Physiological Reviews*, *99*(1), 665–706. https://doi.org/10.1152/physrev.00067.2017

Russo, E., & Villa, C. (2019). Poloxamer hydrogels for biomedical applications. *Pharmaceutics*, *11*(12), 671. https://doi.org/10.3390/pharmaceutics11120671

Sharma, A., Khanna, S., Kaur, G., & Singh, I. (2021). Medicinal plants and their components for wound healing applications. *Future Journal of Pharmaceutical Sciences*, *7*(1), 53. https://doi.org/10.1186/s43094-021-00202-w

Soni, A., & Sosa, S. (2013). Phytochemical analysis and free radical scavenging potential of herbal and medicinal plant extracts. *Journal of Pharmacognosy and Phytochemistry*, *2*(4), 22–29.

Wilkinson, H. N., & Hardman, M. J. (2020). Wound healing: Cellular mechanisms and pathological outcomes. *Open Biology*, *10*(9), 200223. https://doi.org/10.1098/rsob.200223

Yaduvanshi, B., Mathur, R., Mathur, S. R., & Velpandian, T. (2011). Evaluation of wound healing potential of topical formulation of leaf juice of *Tridax procumbens* L. in mice. *Indian Journal of Pharmaceutical Sciences*, *73*(3), 303–306. https://doi.org/10.4103/0250-474X.93523